Biomed Microdevices (2006) 8:263–269
DOI 10.1007/s10544-006-9144-x

DNA counterion current and saturation examined by a MEMS-based solid state nanopore sensor

Hung Chang · Bala Murali Venkatesan · Samir M. Iqbal · G. Andreadakis · F. Kosari · G. Vasmatzis · Dimitrios Peroulis · Rashid Bashir

Published online: 23 June 2006

Abstract Reports of DNA translocation measurements have been increasing rapidly in recent years due to advancements in pore fabrication and these measurements continue to provide insight into the physics of DNA translocations through MEMS based solid state nanopores. Specifically, it has recently been demonstrated that in addition to typically observed current blockages, enhancements in current can also be measured under certain conditions. Here, we further demonstrate the power of these nanopores for examining single DNA molecules by measuring these ionic currents as a function of the applied electric field and show that the direction of the resulting current pulse can provide fundamental insight into the physics of condensed counterions and the dipole saturation in single DNA molecules. Expanding on earlier work by Manning and others, we propose a model of DNA counterion ionic current and saturation of this current based on our experimental results. The work can have broad impact in understanding DNA sensing, DNA delivery into cells, DNA conductivity, and molecular electronics.

H. C. and B. M. V. contributed equally to the work.

H. Chang · B. M. Venkatesan · S. M. Iqbal · D. Peroulis
Birck Nanotechnology Center, School of Electrical and Computer Engineering, Purdue University, West Lafayette, IN, USA

G. Andreadakis · F. Kosari · G. Vasmatzis
Department of Laboratory Medicine and Pathology, Division of Experimental Pathology, Mayo Clinic, Rochester, MN, USA

R. Bashir (✉)
Birck Nanotechnology Center, School of Electrical and Computer Engineering, Weldon School of Biomedical Engineering, School of Mechanical Engineering, Purdue University, West Lafayette, IN, USA
e-mail: bashir@purdue.edu

Keywords Nanopore · DNA counterions · Single molecule

1. Introduction

The sensing and characterization of DNA molecules using nanometer sized solid state pores is fast becoming a reality due primarily to advances in the methods available for pore fabrication (Li et al., 2001; Storm et al., 2003; Chang et al., 2006). Solid state nanopores continue to provide new insight into the physics of DNA translocations through nanopores. These sensors can be more robust, able to operate in various pHs, chemically stable, and easily tuned to the desired sizes. Consequently, measurements have been reported on DNA translocation, folding and conformational changes (Li et al., 2003; Chen et al., 2004; Storm et al., 2005a; Storm et al., 2005b), measurements at high pH (Fologea et al., 2005a), at low temperatures (Fologea et al., 2005b), with multiple DNA lengths (Heng et al., 2004), under high strength of electric fields (Heng et al., 2005), and with surface modified by atomic layer deposition (ALD) (Chen et al., 2004). Due to the complex interactions among DNA, counterions, and nanopores, the device physics is still unclear and unexpected results have been reported, for example, it has been shown that the nanopore sensor can be operated in additional detection modalities than a conventional 'molecular coulter counter', i.e. detection of DNA only due to the physical blocking of the background ionic current. Conductivity of the particle translocating the pore itself was postulated to impact the direction of the pulses (Bezrukov, 2000). Subsequently, it was shown that at low concentration of KCl in the solution, the current can actually increase when the DNA traverses the pore (Chang et al., 2004; Fan et al., 2005; Smeets et al., 2006) and this increase in current has been attributed to the

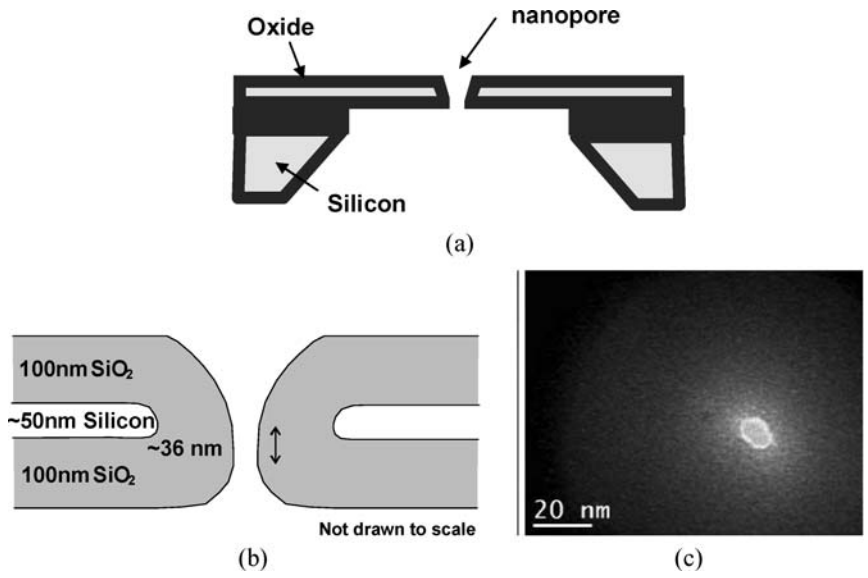

Fig. 1 (a) Drawn schematic of the oxidized membrane in a silicon wafer, (b) close up of the nanopore channel region, and (c) TEM image of the pore used in the measurements with size of $\sim$ 10 nm diameter

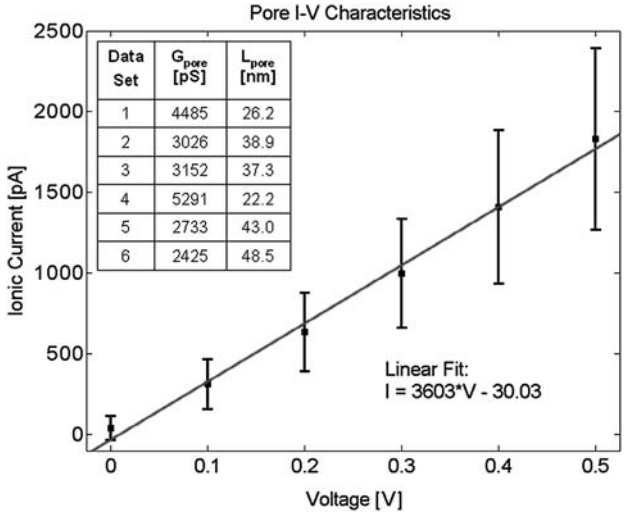

Fig. 2 I-V characteristics of nanopore of diameter 10 nm. Measurements were done with KCl buffer solution of molarity 0.1 M in the absence of DNA. 6 sets of I–V data were taken with calculated conductances and pore lengths summarized in the table inset in Fig. 2. A linear fit was done on the extracted data to obtain pore conductance and an average pore length of 36 $\pm$ 10 nm

movement of potassium ions in the counter-ion charge shielding layer around the DNA. This enhancement current dominates at low background KCl concentrations and becomes smaller than the background ionic current above a critical KCl concentration, which has been calculated and measured to be close to 0.4 M. In our work here, we show that the measurement of current enhancement and blocking can provide fundamental insight into single molecule biophysics. At low molarity and low applied voltages, current enhancements are observed upon DNA translocation due to the counterions around the DNA. However, as the voltage is increased, we show that these pulses can reverse directions, indicating the first experimental observations of saturation of this counterion current in single DNA molecules. The measurements provide another means to probe the concept of DNA polarization and the saturation of these field induced charge dipoles as introduced by Manning (Manning, 1978; Manning, 1993). The saturation of the enhancement current causes a reversal in the pulse direction of DNA-induced translocation events, occurring at voltages larger than a threshold voltage V_T, which is inversely dependent on the background KCl molarity. The saturation in the counterion current can be considered analogous to the channel pinch-off in semiconductor field-effect transistors.

2. Experimental procedures

The nanopores used in our measurements were fabricated as reported earlier (Chang et al., 2004). Figure 1 shows a drawn cross-section of the nanopore and the corresponding TEM image, showing the diameter to be approximately 10 nm. Pore length was determined by taking a series of ionic current-voltage measurements on the same nanopore using KCl buffer solution of molarity 0.1 M, illustrated in Fig. 2. The current-voltage characteristics were used to first calculate pore conductance assuming the effects of surface charge were negligible. This assumption needs to be treated with care. The point of zero charge (PZC) for silanol groups present on the oxide surface of the pore is approximately 3 (Raiteri et al., 1998). The aqueous KCl buffer solutions used in these experiments were of pH 8.5, notably higher than the PZC of silanol groups. Thus significant deprotonation of surface sites, resulting in fixed oxide charge is expected. However, as a first order approximation of channel length, the bulk conductance model is applicable (see Fig. 2 in Smeets et al., 2006). Using

this bulk conductance model, we calculated our pore lengths to be ∼36 ± 10 nm. Three KCl concentrations were prepared for the voltage dependent measurements: 0.1, 0.3, and 0.7 M. The DNA fragment (1691 bp) in the experiments was prepared by PCR amplification of a commercially available vector containing the CRISP-3 sequence (Catalogue ID: H-X94323 M, Invitrogen, Carlsbad, CA) followed by purification of the PCR product. The purified DNA was used at concentration of 133 ng/μl and introduced on one side of the nanopore, in experimental setup as described earlier (Chang et al., 2004).

3. Results and discussions

Figure 3 shows typical pulse streams obtained during our measurements with a 1691 base long dsDNA molecule introduced on one side of the membrane with the nanopore. As shown in Figs. 3(a)–(c), when the molarity is higher than about 0.3 M, the pulses are as expected from the classical 'coulter counter' blockages, even with increasing voltage. The surprising and unexpected behavior was observed when at lower molarities, the electrophoretic bias voltage was increased. At 0.1 M KCl, the pulses are upwards at 0.2 V (Fig. 3(d)), whereas at 0.3 V both downwards and upwards pulses were observed (Fig. 3(e)). At 0.4 V (and at 0.5 V, pulse stream not shown), the pulses were seen to completely reverse in direction (Fig. 3(f)). As shown in more detail in Fig. 4(a), at 0.2 V, 100% of the pulses are upwards at 0.1 M and 0.3 M, whereas 100% of the pulses are downwards at 0.7 M. As the voltage is increased to 0.3 V, the majority of the pulses are still upwards for 0.1 M, while at 0.3 M, majority of the pulses are now downwards. Similarly at 0.4 V majority of the pulses are downwards and finally at 0.5 V, all pulses are downwards for all molarities measured. Figure 4(b) shows a scatter plot of pulse amplitude versus pulse duration, again showing the change in pulse direction with increasing voltage. The average pulse amplitude as a function of voltage shows a transition from upwards to downwards at around $V_T \sim 0.27$ V at 0.3 M and at $V_T \sim 0.34$ V at 0.1 M.

The current through the pore can be expressed as,

$$I_{pulse} = I_{DNA} + I_{enhancement} - I_{blocking}, \quad (1)$$

where, $I_{enhancement}$ is the current contribution of condensed counterions on DNA, and $I_{blocking}$ is the current reduction due to the DNA mechanically blocking the background ionic currents. Positive values suggest upwards pulses in this equation. It should be noted that the current due to the movement of the DNA itself, I_{DNA}, can be neglected since the mobility of the DNA is 3–4 orders of magnitude smaller than the mobility of the ions. Substituting parameters in place of the $I_{enhancement}$ and $I_{blocking}$ terms in the above equation, the current pulse due to the translocation of a single DNA molecule can be written as:

$$I_{pulse} = k(V_{bias}/L_{pore})2q(1-\varphi)\mu_{K+int}/b - k(V_{bias}/L_{pore})qM^*(\mu_{K+} + \mu_{Cl-})A_{pore}, \quad (2)$$

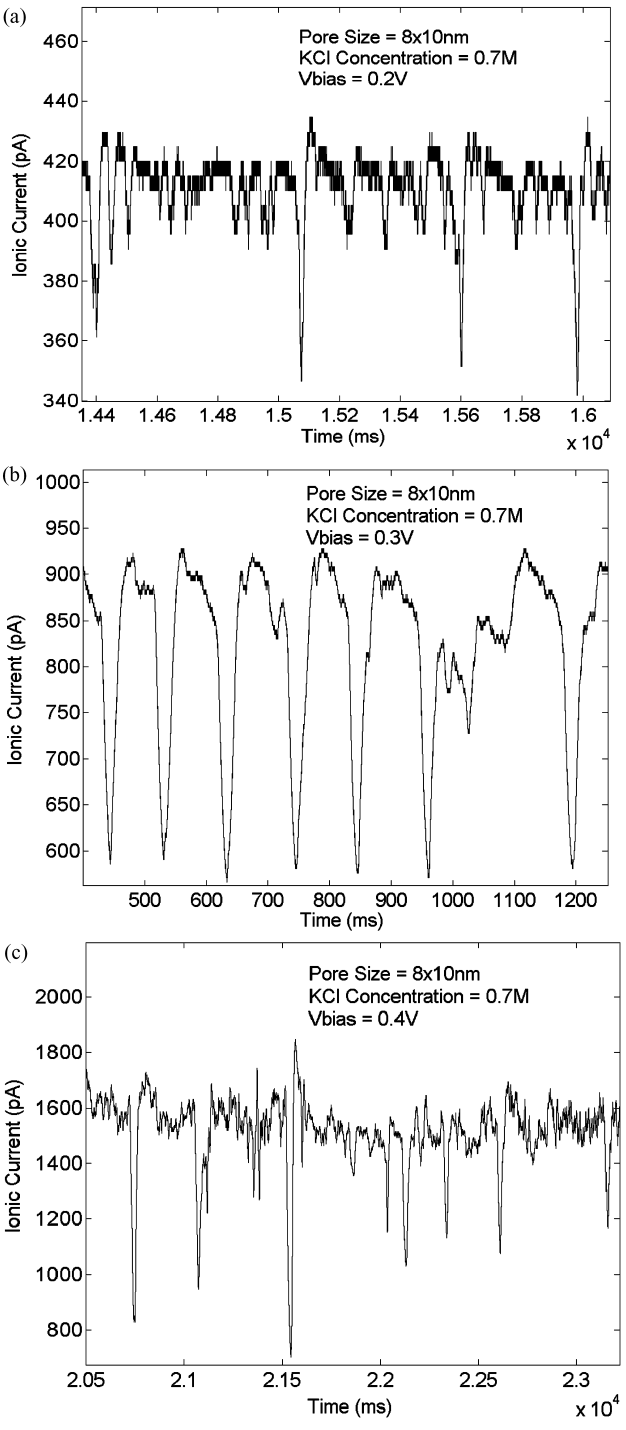

Fig. 3 Voltage dependent reversal of pulse direction, (a)–(c) show that at 0.7 M the pulse direction does not change with increase in voltage, (d)–(f) show the change in pulse direction as the voltage is increased from 0.2 to 0.4 Volts at 0.1 M

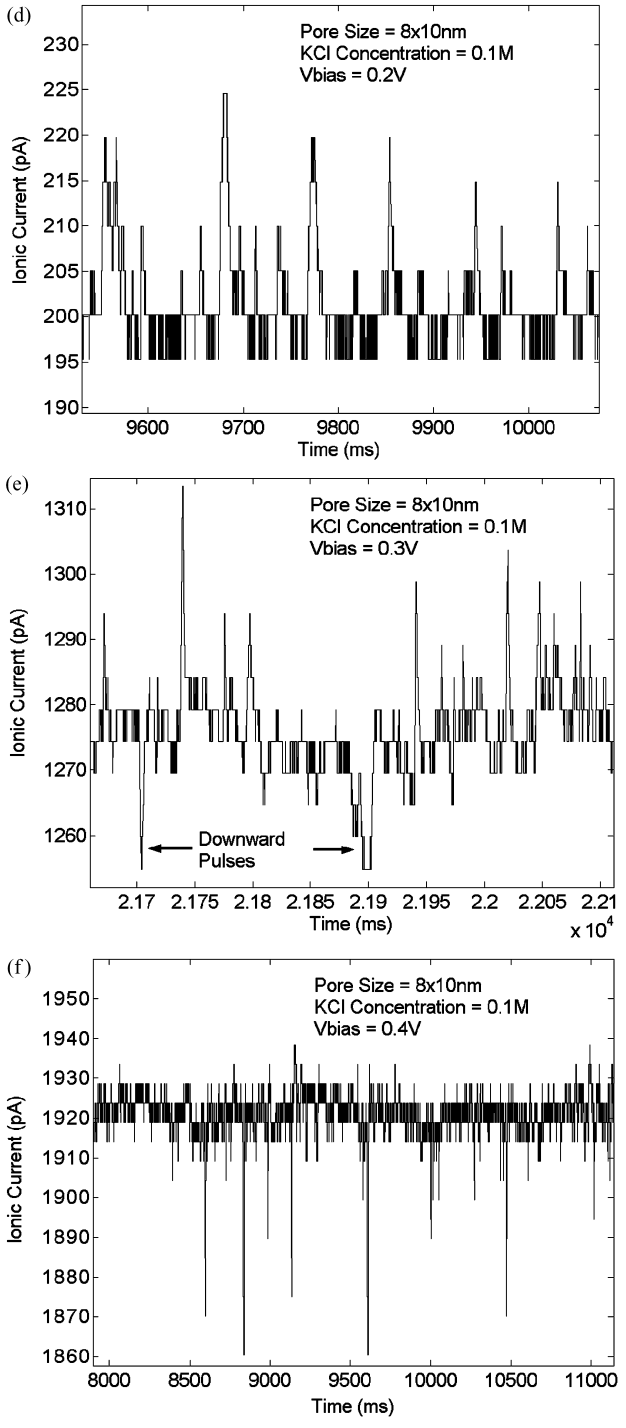

Fig. 3 (*cont.*)

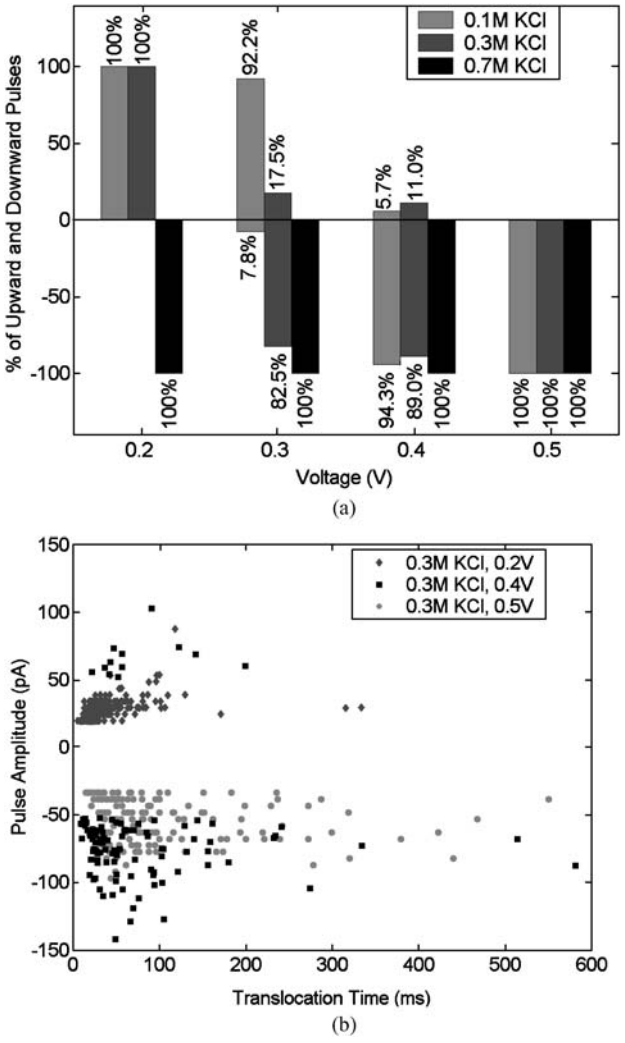

Fig. 4 (a) Percentage of pulses in upward and downward directions at each KCl concentration with increase in voltage. As is clearly demonstrated, at 0.1 M and 0.3 M, all the pulses are up at 0.2 V and eventually all become downwards at 0.5 V. At 0.7 M, for example, the pulses always stay in the downward direction, (b) Scatter plot of pulse amplitude versus pulse direction for 0.2, 0.4, and 0.5 Volts, all 0.3 M, showing the pulse change direction with increasing voltage

where k is the fraction of the total voltage that is dropped across the nanopore, V_{bias}/L_{pore} is the applied electric field, ϕ is the fraction of DNA ionization from Manning's condensation theory (Manning, 1978; Manning, 1993), μ_{K+int} is the potassium counterion mobility around the DNA, b is the linear distance between the bases in a DNA molecule, μ_{K+} and μ_{Cl-} are potassium and chloride ion mobilities in bulk solution respectively, M^* is concentration per unit volume of the K^+ and Cl^- ions (proportional to molarity of KCl), and A_{pore} is the cross section of the pore.

It can be seen that from the equation above, the voltage dependence of both components is the same, so why do the current pulses reverse direction with voltage? Our results indicate that the blocking current becomes larger than the enhancement current as the bias is increased above a threshold voltage V_T, and the pulse direction reverses. These results can be explained if the earlier theoretical work is examined and consolidated to present a unified model as follows. Manning (Manning, 1993) and others (Oosawa, 1971; Mandel, 1961; Netz et al., 2003; Lansac et al., 2004; O'Shaughnessy

et al., 2005; Diekmann et al., 1982; Diekmann et al., 1984; Porschke, 1985) examined the effect of electric field on DNA counterion condensation, polarization, and mobility. Manning's model assumes that in the case of no electric field, the ratio of shielded charges to total charges on the DNA is $1-\phi = kTb\varepsilon/(Nq^2) = 0.76$, where k is Boltzmann's constant, T is temperature in Kelvin, b is the average space between backbone phosphates (which is 0.17 nm for B-DNA), ε is the dielectric constant of the solvent, q is electronic charge, and N is the valency of counterions (1 for K^+ ions). However, when a longitudinal electric field is applied across the DNA, the condensed counterions start to move from one side of the DNA molecule to the other, resulting in the formation of a dipole. Even though the distribution of condensed counterions can be non-uniform, Manning's theoretical analysis assumed that their amount $2qN(1-\phi)L_{DNA}/b$, remains the same with increasing electric field strength. At high fields, the end of the DNA close to the anode gets 'depleted' of the condensed counterions. Conversely, the counterions accumulate at the other end, which gets 'augmented'. Thus, the DNA is polarized but the counterions do not conduct until a saturation electric field, E_{sat} is reached, above which, the charge dipole is saturated and further increase in electric field results in current flow. However, it should be noted that the counterions can be in two states depending on their distance from polyelectrolytes (PE): mobile and bound (Oosawa, 1971; Mandel, 1961; Netz et al., 2003; Lansac et al., 2004; O'Shaughnessy et al., 2005). Oosawa (Oosawa, 1971) described that for a coiled polymer chain, counterions located at one of three positions can be considered condensed while the counterions in the remaining two regions maybe considered as mobile. Keeping the fact in mind that there are mobile counterions available in addition to the ones that are very tightly bound, we hypothesize, that the current due to the counterions can start to flow as soon as even a small voltage is applied, as schematically shown in Fig. 5, and the activation energy barrier to this current flow is much smaller than the $E_{\rm sat}$. The current flow and counterion depletion is depicted in our model in Figs. 5(a)–(c). As also shown in Figs. 5(d) and (e), if the background ionic blocking current (2nd component in the current equation above) is small, than the enhancement current will dominate and we measure pulses in the upward direction. As the applied voltage is increased, eventually we reach the point E_{sat}, where the DNA dipole is saturated and there is a region in the DNA close to the anode which is completely depleted of the counterions, analogous to the channel pinch off in a field effect transistor. At this point, the enhancement current due to the counterions will saturate, the current pulses will start to reverse direction and we believe this applied electric field to be equal to or larger than the saturation field.

There is also much discrepancy on the value of the saturation electric field, ε_{sat}, in previous reports. In his theoretical study (Manning, 1993), Manning defined a dimensionless electric field $\varepsilon = (q/\mathrm{kT}) \cdot (V/L_{pore}) \cdot L_{\rm DNA}$, where E is applied electric field and L_{DNA} is the molecule length under investigation. Manning's simulation arrived at the saturation electric field to be $\varepsilon_{sat} > 90$ (and noted that this was overestimated), which for our case correspond to $V_{sat} \sim 2.3$ V ($E_{sat} \sim 6.5 \cdot 10^5$ V/cm), about 7-8 times larger than the voltage where we see the pulse direction reverse. Earlier theoretical work (Mandel, 1961) estimated $\varepsilon_{sat} \sim 15$ which for our case would be ~ 0.39 V ($E_{sat} \sim 1.1 \cdot 10^5$ V/cm). The only experimental results to date from electrical dichroism measurements (Diekmann et al., 1982; Diekmann et al., 1984; Porschke, 1985) showed that the saturation electric field for ~100 bp long molecule was measured to be $E_{sat} \sim 2 \cdot 10^4$ V/cm, corresponding to Manning's $\varepsilon_{sat} \sim 2.3$ and $V_{sat} \sim 0.06$ V for our experimental case). Hence, our measurements are in agreement with these prior experimental results and we would thus propose that the counterion enhancement current be written as;

$$I_{enhancement} = k(V_{bias}/L_{pore})q(1-\varphi)\mu^+_{Kint}/b;\ for\ V_{bias} < V_{sat}$$

$$I_{enhancement} = k(V_{sat}/L_{pore})q(1-\varphi_{sat})\mu^+_{Kint}/b;\ for\ V_{bias} > V_{sat}$$

As shown schematically in the model in Fig. 5(d), at high molarities, the blocking current would dominate and the pulses would be downwards, but as the molarity is decreased, the enhancement current would dominate. However, as the voltage is increased at lower molarities to a threshold voltage V_T, the blocking current can dominate again. It should be noted that the enhancement current could also possibly decrease, indeed, simulations studies have shown the possibility of decrease of the total counterions by 20–40% with increasing electric field in the range of our experimental conditions (Netz et al., 2003; Lansac et al., 2004). However, from the same computational studies, the effective mobility of the counterions is shown to initially increase and then decrease with increasing electric fields by about the same degree at high fields. So the net effect of the $(1-\phi)x\mu^+_{Kint}$ preduct with increasing voltage is more difficult to analyze. More detailed measurements at finely spaced voltages and molarities with the nanopore can provide an answer to this question, a task underway in our group.

4. Conclusions

In summary, we use ionic current measurements through solid state nanopores during DNA translocations to show for the first time, that at low ionic concentrations, the measured current direction can reverse with increasing voltage due to competition between the blocking current and the counterion

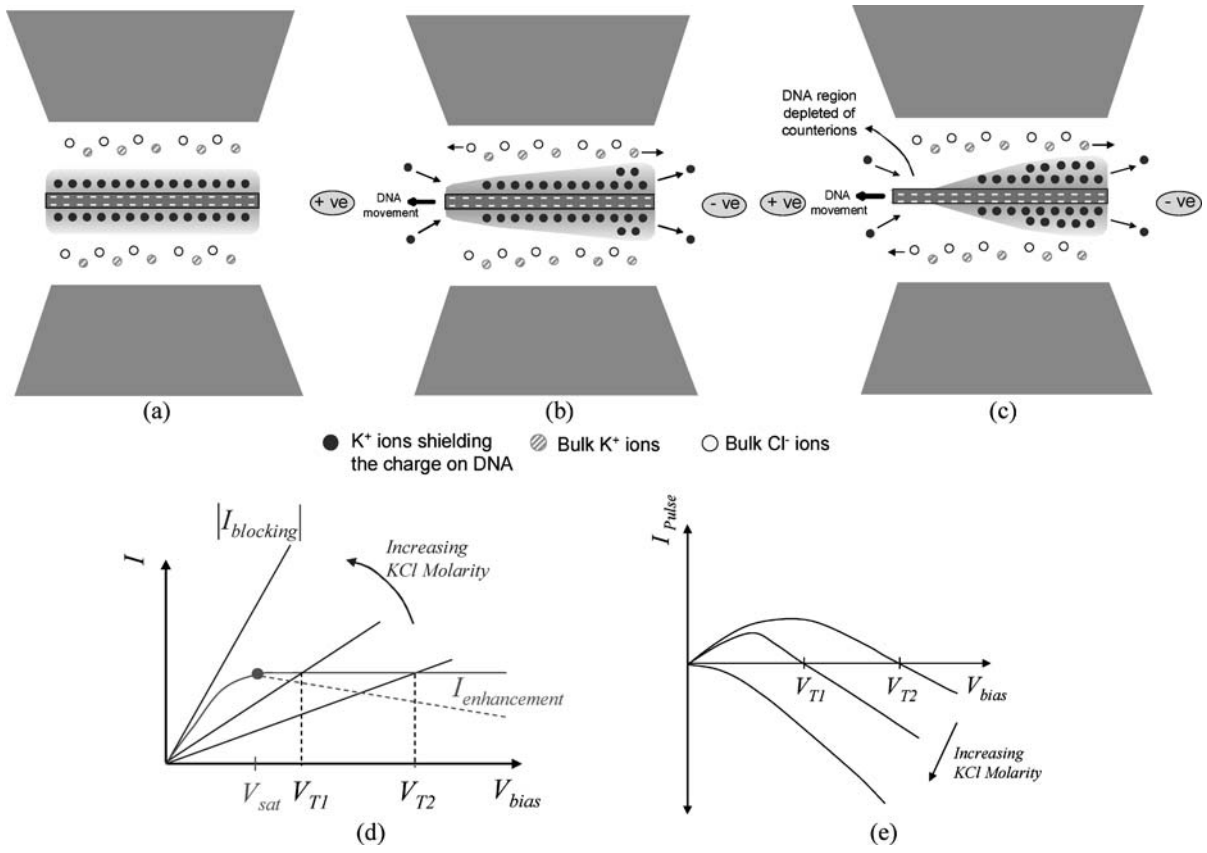

Fig. 5 Schematic of the current components in the pore and the ionic current flow around the DNA inside the nanopore. (a) when no electric field is applied, the counterions are distributed uniformly around the DNA, (b) at low electric fields $V_{app} < V_{sat}$, the mobile counterions start to move and potassium ionic current starts to flow and the DNA starts to polarize, (c) at high electric fields $V_{app} > V_{sat}$, the end of the DNA closest to the anode gets depleted of the counterions and a 'pinched off' region is created, analogous to a field effect transistor and the enhancement current saturates, (d) proposed model of the enhancement and blocking current variation versus electric field and molarity, the counterion current can saturate or decrease based on whether the product of counterion mobility and ionization saturates or decreases, (e) proposed model of the net measured current as a function of electric field and molarity. It should be noted that the nanopore oxide sidewalls can also have a negative charges which can accumulate a potassium ion current close to the sidewall, resulting in an electroosmotic current which can add to the measured current

current, latter saturating at high electric field. We also show that our data is consistent with the previously measured electrical dichroism measurements and that the nanopore sensors provide a direct means to explore the charge polarization and dipole saturation at the single molecule level.

5. Acknowledgments

We would like to thank the NASA Institute for Nanoelectronics and Computing (INAC) at Purdue under award no. NCC 2-1363 for funding the work. We also want to thank Edward Basgall at The Pennsylvania State University for electron beam lithography through the NSF-funded National Nanotechnology Infrastructure Network (NNIN). Partial wafer fabrication was performed at Nanotechnology Core Facility at University of Illinois at Chicago.

References

S.M. Bezrukov, Journal of Membrane Biology **174**, 1 (2000).
H. Chang, F. Kosari, G. Andreadakis, M.A. Alam, G. Vasmatzis, and R. Bashir, Nano Letters **4**, 1551 (2004).
H. Chang, S.M. Iqbal, E.A. Stach, A.H. King, N.J. Zaluzec, and R. Bashir, Applied Physics Letters **88**, 103109 (2006).
P. Chen, T. Mitsui, D.B. Farmer, J. Golovchenko, R.G. Gordon, and D. Branton, Nano Letters **4**, 1333 (2004).
P. Chen, J. Gu, E. Brandin, Y. Kim, Q. Wand, and D. Branton, Nano Letters **4**, 2293 (2004).
S. Diekmann, W. Hillen, M. Jung, R.D. Wells, and D. Porschke, Biophysic Chemistry **15**, 157 (1982).
S. Diekmann, M. Jung, and M.J. Teubner, Journal of Chemical Physics **80**, 1259 (1984).
R. Fan, K. Rohit, M. Yue, D. Li, A. Majumdar, and P. Yang, Nano Letters **5**, 1633 (2005).
D. Fologea, M. Gershow, B. Ledden, D.S. McNabb, J.A. Golovchenko, and J. Li, Nano Letters **5**, 1905, (2005a).
D. Fologea, J. Uplinger, B. Thomas, D.S. McNabb, J. Li, Nano Letters **5**, 1734 (2005b).

J.B. Heng, C. Ho, T. Kim, R. Timp, A. Aksimentiev, Y.V. Grinkova, S. Sligar, K. Schulten, and G. Timp, Biophysics Journal **87**, 2905 (2004).
J.B. Heng, A. Aksimentiev, C. Ho, P. Marks, Y.V. Grinkova, S. Sligar, K. Schulten, and G. Timp, Nano Letters **5**, 1883 (2005).
Y. Lansac, P.K. Maiti, and M.A. Glaser, Polymer **45**, 3099 (2004).
J. Li, D. Stein, C. McMullan, D. Branton, M.J. Aziz, and J.A. Golovchenko, Nature **412**, 166 (2001).
J. Li., M. Gershow, D. Stein, E. Brandin, and J.A. Golovchenko, Nature Materials **2**, 611 (2003).
M. Mandel, Molecular Physics **4**, 489 (1961).
G.S. Manning, Quarterly Reviews of Biophysics **11**, 179 (1978).
G.S. Manning, Journal of Chemical Physics **99**, 477 (1993).
R.R. Netz, Journal of Physical Chemistry B. **107**, 8208 (2003).
B. O'Shaughnessy, and Q. Yang, Physical Review Letters **94**, 048302 (2005).
F. Oosawa, Polyelectrolytes, Marcel Dekker, New York (1971).
D. Porschke, Biophysical Chemistry **22**, 236 (1985).
R. Raiteri, B. Margesin, and M. Grattatola, Sensors and Actuators, B. **46**, 126 (1998).
R.M.M. Smeets, U. Keyser, D. Krapf, M. Wu, N.H. Dekker, and C. Dekker, Nano Letters **6**, 89 (2006).
A.J. Storm, J.H. Chen, X.S. Ling, H.W. Zandbergen, and C. Dekker, Nature Materials **2**, 537 (2003).
A.J. Storm, J.H. Chen, H.W. Zandbergen, and C. Dekker, Physical Review E **71**, 051903 (2005a).
A.J. Storm, J.H. Chen, H.W. Zandbergen, J-F. Joanny, and C. Dekker, Nano Letters **5**, 1193 (2005b).